Preclinical and Clinical Pharmacology of Basmisanil, a Novel Selective $GABA_A$-α5 Receptor Negative Allosteric Modulator

Joerg Hipp[1], Frédéric Knoflach[1], Robert Comley[1], Theresa Ballard[1], Michael Honer[1], Gerhard Trube[1], Rodolfo Gasser[1], Eric P. Prinssen[1], Tanya Wallace[1], Andreas Rothfuss[1], Henner Knust[1], Sian Lennon-Chrimes[1], Michael Derks[1], Lisa Squassante[1], Stephane Nave[1], Jana Noeldeke[1], Christoph Wandel[1], Andrew Thomas[1], and Maria-Clemencia Hernandez[1]

[1]F Hoffmann-La Roche AG Research and Development Division

July 16, 2020

Abstract

Background and Purpose $GABA_A$-α5 subunit-containing receptors have been shown to play a key modulatory role in cognition and represent a promising drug target for cognitive dysfunction, as well as other disorders. We describe the preclinical and clinical profile of basmisanil, a potent and highly selective negative allosteric modulator (NAM) of $GABA_A$ α5 receptors. Experimental Approach In vitro assays assessed binding and functional selectivity. In vivo occupancy studies measured target engagement. Effects on cognition were tested in rats (Morris water maze) and non-human primates (NHP; object retrieval) and potential side effects (anxiety and proconvulsant) were tested in rats. In healthy volunteers, target engagement and modulation of neuronal network activity were assessed using PET and EEG. Key Results Basmisanil bound to recombinant human $GABA_A$-α5 receptors with 5 nM affinity and more than 90-fold selectivity versus α1, α2, and α3 subunit-containing receptors. Basmisanil inhibited GABA-induced currents at $GABA_A$-α5 yet had little or no effect at the other receptor subtypes. In vivo, basmisanil demonstrated dose-dependent target engagement in rats. Basmisanil attenuated diazepam-induced spatial learning impairment in rats and improved executive function in NHPs. At these efficacious plasma concentrations, basmisanil had no anxiogenic and proconvulsant effects. In healthy volunteers, PET showed target engagement and established the plasma exposure to receptor occupancy relationship. Basmisanil modulated brain function reflected in characteristic changes of EEG spectral power. There were no serious adverse events. Conclusion and Implications Basmisanil is a highly potent and selective $GABA_A$ α5 receptor NAM with good safety and tolerability allowing for clinical testing in multiple brain disorders.

Title

Preclinical and Clinical Pharmacology of Basmisanil, a Novel Selective $GABA_A$-α5 Receptor Negative Allosteric Modulator

Short running title

Basmisanil, a highly selective $GABA_A$-α5 NAM

Full names of all authors

Joerg F Hipp[1], Frederic Knoflach[1], Robert Comley[1], Theresa M. Ballard[1], Michael Honer[1], Gerhard Trube[1], Rodolfo Gasser[2], Eric Prinssen[1], Tanya L. Wallace[5], Andreas Rothfuss[2], Henner Knust[3], Sian Lennon-

Chrimes[4], Michael Derks[4], Lisa Squassante[4], Stephane Nave[1], Jana Nöldeke[1], Christoph Wandel[2], Andrew W Thomas[3], Maria-Clemencia Hernandez[1]

All authors institutional affiliations (where work was carried out)

[1] Neuroscience & Rare Diseases (NRD) Discovery and Translational Area

[2] Pharmaceutical Sciences

[3] Small Molecule Research

Roche Pharmaceutical Research and Early Development, Roche Innovation Center Basel, Grenzacherstrasse 124, 4070 Basel, Switzerland.

[4] Pharmaceutical Sciences, Roche Pharma Research and Early Development, Roche Innovation Center Welwyn, Welwyn Garden City, AL7 1TW, UK.

[5] CNS Research, Roche Bioscience, Palo Alto, USA

Current Affiliation

TLW: BlackThorn Therapeutics, 780 Brannan Street, San Francisco, California 94103, USA

TMB: Galwyn (UK) Ltd, Dartmouth, Devon, UK.

AWT: Helvetica Capital AG, Zurich, Switzerland.

RC: AbbVie Inc, North Chicago, Illinois, USA.

Word count: 3996 (excluding abstract, methods, references and figure legends):

- Introduction: 660
- Results: 1838

Discussion & Conclusions: 1498

Abstract: 250

Acknowledgements

The authors thank Gregoire Friz, Cecile Guizani, Marie-Laurence Harle-Yge and Maria Karg (molecular biology, binding assays), Pascal Pflimlin and Veronique Graf (*Xenopus* oocyte in-vitro electrophysiology), Brigitte Algeyer, Severine Bandinelli, Gabriel Chiu, Hung Dao, Marie Haman, Francoise Kahn and Roger Wyler (behavioural pharmacology), Nicholas Seneca (neuroscience development), Elisabeth Husar, Theo Dinklo, Andrea Greiter-Wilke, Björn Jacobsen, Monique Schmitt and Erich Wolz (pharmaceutical sciences), Andreas Koblet, Anke Kurt, Heidi Schaer, Pius Waldmeier (chemistry), Nicole Wyttenbach (drug product), Candice Jamois, Cheikh Diack and Darren Bentley (clinical pharmacology), Andrew P. Brown, Graham E. Searle, Roger N. Gunn, Eugenii A. Rabiner (PET study, Imanova Ltd.).

Conflicts of interest statement

All authors were employees of F.Hoffmann-La Roche AG Switzerland or Roche Bioscience USA or Roche Products Ltd. UK at the time of the preclinical and clinical studies.

Abstract

Background and Purpose

$GABA_A$-α5 subunit-containing receptors have been shown to play a key modulatory role in cognition and represent a promising drug target for cognitive dysfunction, as well as other disorders. We describe the preclinical and clinical profile of basmisanil, a potent and highly selective negative allosteric modulator (NAM) of $GABA_A$-α5 receptors.

Experimental Approach

In vitro assays assessed binding and functional selectivity. In vivo occupancy studies measured target engagement. Effects on cognition were tested in rats (Morris water maze) and non-human primates (NHP; object retrieval) and potential side effects (anxiety and proconvulsant) were tested in rats. In healthy volunteers, target engagement and modulation of neuronal network activity were assessed using PET and EEG.

Key Results

Basmisanil bound to recombinant human $GABA_A$-α5 receptors with 5 nM affinity and more than 90-fold selectivity versus α1, α2, and α3 subunit-containing receptors. Basmisanil inhibited GABA-induced currents at $GABA_A$-α5 yet had little or no effect at the other receptor subtypes. In vivo, basmisanil demonstrated dose-dependent target engagement in rats. Basmisanil attenuated diazepam-induced spatial learning impairment in rats and improved executive function in NHPs. At these efficacious plasma concentrations, basmisanil had no anxiogenic and proconvulsant effects. In healthy volunteers, PET showed target engagement and established the plasma exposure to receptor occupancy relationship. Basmisanil modulated brain function reflected in characteristic changes of EEG spectral power. There were no serious adverse events.

Conclusion and Implications

Basmisanil is a highly potent and selective $GABA_A$-α5 receptor NAM with good safety and tolerability allowing for clinical testing in multiple brain disorders.

Bullet point summary

What is already known

Genetic and pharmacological studies have demonstrated the importance of $GABA_A$-α5 subunit-containing receptors on cognition.

What this study adds

- Basmisanil is the most potent and highly selective $GABA_A$-α5 negative allosteric modulator described so far.
- Basmisanil showed dose-dependent target engagement (rats, humans) and pharmacodynamic effects preclinically (cognition) and clinically (EEG).

Clinical significance

- Basmisanil shows good safety and tolerability in humans at maximum $GABA_A$-α5 receptor occupancy.
- Basmisanil has an ideal profile to investigate potential clinical benefits of $GABA_A$-α5 receptor negative modulation.
-

Keywords

Basmisanil, $GABA_A$-α5, Cognition, PET, EEG

1 Introduction

$GABA_A$ receptors are a family of ligand-gated ion channels which respond to the major inhibitory neurotransmitter, GABA. There are 19 genes encoding for $GABA_A$ receptor subunits that assemble as pentamers, with the most common stoichiometry of two α, two β, and one γ subunit (Olsen & Sieghart, 2009). GABA has two binding sites at the interface of the α and β subunits. Many compounds in clinical use as anxiolytics, sedatives, hypnotics or antiepileptics bind to the allosteric benzodiazepine (BZD) binding site which is formed by one of the α subunits (α1, α2, α3 or α5) and usually the γ2 subunit. These compounds are known as positive allosteric modulators (PAMs) since they have no effect alone, but increase the activity of $GABA_A$receptors in the presence of GABA (Sieghart & Savic, 2018; Sigel & Steinmann, 2012). In contrast, negative allosteric modulators (NAMs) are BZD-binding site ligands which decrease the activity of $GABA_A$ receptors, have not been successfully developed today.

Both genetic and pharmacological studies have demonstrated that $GABA_A$-α5 subunit-containing receptors play an important modulatory role in learning and memory processes, in line with their preferential expression in the hippocampus and cortical regions (Rudolph & Knoflach, 2011). Several compounds have been described to possess selectivity for the α5 containing receptors and in preclinical studies have demonstrated cognitive enhancement without the anxiogenic or proconvulsant side effects associated with non-selective NAMs (Dorow et al., 1983; Little etal., 1984), such as, α5IA (Dawson et al., 2006), MRK-016 (Atack et al., 2009), PWZ-029 (Savic et al., 2008), RO4938581 (Ballard et al., 2009), ONO-8290580 (Kawaharada et al., 2018).

Initially, it was proposed that selective $GABA_A$-α5 NAMs may be beneficial for Alzheimer's Disease and mild cognitive impairment (Maubach, 2003). Since then, further preclinical studies suggest that $GABA_A$-α5 NAMs may attenuate cognitive impairment associated with Down syndrome (Braudeau et al., 2011; Martinez-Cue et al., 2013), cognitive impairment associated with schizophrenia as shown by improvements in preclinical models of NMDA dysfunction (Povroznik etal., 2014; Redrobe et al., 2012; Timic Stamenic et al., 2015) and cognitive impairment after anesthesia (Zurek et al., 2014). In addition, studies in mice and rats have shown that after ischemic stroke there is increased $GABA_A$-α5 mediated tonic inhibition in the peri-infarct area and that reduction of $GABA_A$-α5 activity enhances functional recovery after stroke (Clarkson etal., 2010; Lake et al., 2015; Schmidt et al., 2012). Recently, $GABA_A$-α5 NAMs have also been shown to exert rapid antidepressant-like effects in mice (Fischell et al., 2015; Zanos et al., 2017).

Therefore, $GABA_A$-α5 NAMs hold promise as potential treatments for multiple indications, particularly associated with cognitive impairment. However, it has not been possible to clinically assess the effects of reduced activity at $GABA_A$-α5 receptors with a selective and safe compound. α5IA and MRK-016 were tested in clinical trials, but their development was stopped because of renal toxicity in preclinical species (Merschman et al., 2005) and poor tolerability in healthy elderly humans as well as variable pharmacokinetics, respectively (Atack, 2010; Atack et al., 2009). RO4938581, had to be abandoned because of strong CYP1A2 autoinduction properties in rats leading to reduced plasma exposure on chronic dosing (Bundgaard et al., 2013), but our continued search for $GABA_A$-α5 selective NAMs without safety liabilities led to basmisanil (**Figure 1**). Basmisanil was discovered in a medicinal chemistry effort starting from the results of a 56,265 small molecular-weight compound library high-throughput screen based on [^{3}H]-flumazenil competition-binding followed by electrophysiological experiments on cloned $GABA_A$ receptor subtypes to determine the functional activity of the initial hits.

The aim of this study was to assess the effects of basmisanil to: (1). establish the relationship between plasma exposure and receptor occupancy in rats (in vivo autoradiography) and humans (PET); (2). calculate esti-

mated receptor occupancy required for in vivo efficacy (improved cognition in rats and non-human primates [NHPs]) compared to side effects (rats); (3). assess CNS activity (EEG) and safety profile in humans.

2 Methods

2.1. In Vitro Studies

For all in vitro studies basmisanil was prepared as a 10 mM stock solution in DMSO.

2.1.1 Radioligand binding assays in HEK293 membrane preparations expressing cloned human $GABA_A$receptors

Plasmids and recombinant cell expression: The cDNAs encoding different human $GABA_A$ receptor subunits (α1-6, β2-3, γ2) were subcloned into the polylinker of the pcDNA3.1 vector (Invitrogene, USA) by standard techniques for transiently transfecting human embryonic kidney (HEK)293-EBNA cells or for in vitro RNA synthesis.

HEK293-EBNA cells adapted to grow in suspension were transiently transfected with the plasmids containing the desired $GABA_A$ receptor subunit cDNAs at α, β, γ, 1:1:2 ratio using XtremeGENEQ2 (Cat. No. 03045595001, Roche Applied Science, RAS, Rotkreuz, Switzerland) as previously described (Malherbe et al., 2008). $GABA_A$ α1β 2γ2, α2β3γ2, α3β3γ2, α4β3γ2, α5β3γ2 and α6β3γ2 receptor subtypes were expressed in this system. 48 h post transfection, the cells were harvested and washed three times with cold PBS and frozen at -80°C.

Membrane preparation and radioligand binding assays: Membrane preparations of HEK293 cells expressing the different $GABA_A$ receptor subtypes and [^{3}H]-flumazenil binding assays were performed as described previously (Ballard et al., 2009). The inhibition of 1 nM [^{3}H]-flumazenil ([^{3}H]RO0151788) binding by basmisanil was measured in membranes expressing human $GABA_A$ α1β2γ2 (n = 9), α2β3γ2 (n = 9), α3β3γ2 (n = 7) and α5β3γ2 (n = 8) receptor subtypes. Non-specific binding was determined in the presence of 10 μM diazepam. The percentage inhibition of [^{3}H]-flumazenil binding, the IC_{50} and the Ki values were calculated using ActivityBase (IDBS; Guildford, Surrey, UK) and as described in the statistical analysis.

The affinity of basmisanil for $GABA_A$ receptors containing α4 and α6 subunits was measured using [^{3}H]-Ro 15-4513 competition-binding experiments. Membranes were incubated with 1 nM of [^{3}H]-Ro 15-4513 and ten concentrations of basmisanil. Nonspecific binding was measured in the presence of 10 μM Ro 15-4513. IC_{50} values were derived from the inhibition curve and Ki values were calculated as described in the statistical analysis section.

2.1.2 Selectivity screening

Binding of basmisanil (10 μM) to 78 other receptors, transporters and channels was tested by Eurofins Cerep SA (Celle l'Evescault, France) following the methods described on the website, www.neurofinsdiscoveryservices.com.

2.1.3 Voltage-clamp of Xenopus laevis oocytes expressing cloned human $GABA_A$receptors

Cloning and preparation of RNA for microinjection into Xenopus laevis oocytes: The cDNAs encoding different human $GABA_A$ receptor subunits were subcloned into the polylinker of the pcDNA3.1 vector (Invitrogene, USA) by standard techniques. The constructs were linearized at the 3' end of the corresponding receptor subunit cDNA with the appropriate restriction enzyme keeping the polymerase promoter site upstream of the sequence to be transcribed (see Supporting Table S1). Capped and poly(A) tailed cRNA transcripts were synthesized from linearized plasmids encoding the desired protein by using the mMessage

mMachine T7 ultra kit (Ambion) according to the recommendation of the manufacturer. The synthesized RNA was purified by using the MEGAclear (Ambion) spin columns. cRNA concentrations were calculated with the Nanodrop 8000 and visualized on 1.5% agarose gels. The RNAs are stored at -80 °C.

Microinjection of oocytes and electrical recording: Freshly prepared oocytes of maturation stage VI were bought from Ecocyte Bioscience (Castrop-Rauxel, Germany) and, after overnight delivery, plated into 96-well plates (Greiner no. 651101) for microinjection on a Roboocyte® R16 system (Multichannel Systems MCS GmbH, Reutlingen, Germany). Each oocyte was injected with roughly 50 nL of RNA solution. The solution for expressing receptors composed of the human α1, β2 and γ2 subunits contained 3 pg/nL of α1 and β2 RNA and 15 pg/nL of γ2 RNA. The solution for expressing human α2β3γ2 receptors contained 2.5 pg/nL of α2 and β3 RNA, 5 pg/nL of γ2 RNA and 10 pg/nL of GABARAP RNA. The solution for expressing human α3β3γ2 receptors contained 1.3 pg/nL of α3 and β3 RNA and 6.5 pg/nL of γ2 RNA. The solution for expressing human α5β3γ2 receptors contained 1.3 pg/nL of α5 and β3 RNA and 13 pg/nL of γ2 RNA. GABARAP was added to the α2β3γ2 subunit mixture since the expression of γ2 would be low otherwise, as indicated by a weak effect of β-CCM (Chen et al., 2005). After the microinjection the oocytes were kept at 20°C temperature until the electrophysiological experiment. Experiments were done 3 to 5 days later on the Roboocyte® instrument which employs the two-microelectrode voltage-clamp technique for membrane voltage control and current measurement. Glass microelectrodes were filled with a mixture of KCl (1 M) and K-acetate (1.5 M) and had a resistance of 0.5 – 0.8 MΩ. During current recording and compound testing the cell membrane was constantly clamped to -80 mV. Current signals were recorded and stored on a PC-type computer using the Roboocyte®software.

Solutions: During the microinjection and up to the electrophysiological experiment the oocytes were kept in a solution containing 88 mM NaCl, 1 mM KCl, 2.5 mM $NaHCO_3$, 10 mM HEPES (AppliChem), 0.82 $MgSO_4$, 0.33 mM $Ca(NO_3)_2$, 0.33 mM $CaCl_2$, 100 U/mL penicillin (GIBCO) and 100 µg/mL streptomycine (GIBCO). The pH was adjusted to 7.5. During the experiment the voltage-clamped oocyte was constantly superfused by a solution containing 90 mM NaCl, 1 mM KCl, 5 mM HEPES (AppliChem), 1 mM $MgCl_2$ and 1 mM $CaCl_2$ (pH 7.4). GABA and test compounds were added to this solution. GABA concentrations were chosen according to previously determined concentration-response relations for the different human $GABA_A$ receptor subunit combinations. Concentrations evoking approximately 10% of a maximal response were selected, i.e., 8 µM for α1β2γ2, 6 µM for α2β3γ2, 10 µM for α2β3γ2 and 5 µM for α5β3γ2. Solutions containing GABA or test compounds were freshly prepared at least every second day. Stock solutions of basmisanil, flumazenil and β-CCM were prepared in DMSO at 10 mM concentration. Compounds were further diluted in DMSO and finally in extracellular saline to reach a DMSO concentration of 0.1%. The same amount of DMSO was added to the control solutions without test compounds.

Compound application: During the experiment the solutions were fed into the well containing the voltage-clamped oocyte via Teflon tubings connected by electromagnetic valves which allowed rapid switching between different solutions (controlled by the Roboocyte® software). Approximately 1–2 min after impaling an oocyte and switching to voltage-clamp mode GABA was applied for 90 s to record a control response. Thereafter the oocyte was washed with saline for 160 s followed by another 90 s GABA application. Then 30 s after the onset of the second GABA application the system switched to a solution containing GABA plus the test compound. Each oocyte was used for testing one concentration of a single test compound (1 nM: n = 3, 10 nM: n = 7, 100 nM: n = 6, 1000 nM: n = 7).

Experiments for testing the antagonism between basmisanil (100 nM: n = 16) and flumazenil (30 nM: n = 5, 1000 nM: n = 11) followed the same general schedule. In this case each GABA application lasted 110 s and the rest period between the two GABA applications was 190 s long. As before, basmisanil was added to the GABA-containing solution 30 s after the onset of the second GABA response and 20 s later the system switched to a solution containing GABA plus basmisanil plus flumazenil (basmisanil + flumazenil 30 nM: n = 6, basmisanil + flumazenil 1000 nM: n = 10).

On each 96-well plate 3-6 oocytes were used for testing a known NAM at the BZD binding site, β-CCM (FG7106), as a positive control. This compound does not discriminate between the different $GABA_A$ receptor

subtypes and thus could be used for all subunit combinations to see if the oocytes were normally responding. Maximally effective concentrations of β-CCM were used for each subunit combination, i.e., 100 nM β-CCM for α1β2γ2, 300 nM for α2β3γ2 or α3β3γ2 and 1 μM for α5β3γ2. The inhibitory effects of β-CCM ranged between 42% and 53% (mean value per plate).

2.2 In Vivo Studies

2.2.1 Animals

Experiments performed at F. Hoffmann-La Roche (Basel) complied with the Swiss Federal and Cantonal laws on animal research and AAALAC regulations and received prior approval by the Cantonal Veterinary Office. The object retrieval task in NHPs was approved by the Roche Palo Alto Institutional Animal Care and Use Committee and were in accordance with the NIH guidelines.

Rats were group housed in separate holding rooms at a controlled temperature (20–23°C), humidity (55-65%) and with a 12 h light/dark cycle. They were allowed ad libitum access to food and water. The animals used in the experiments were Wistar rats (PTZ experiments: 200-220 g, male and female), Sprague-Dawley rats (receptor occupancy: 180 g, female; stimulus rat for social approach avoidance test: 450-500 g, male), Lister Hooded rats (Morris water maze: 220-250 g, male), F-344 Fischer rats (social approach avoidance test: 170-180 g, male).

Male cynomolgus macaques (Macaca fascicularis; 7-10 kg; Charles River, Houston TX) were fed their full daily regimen of food (Purina High Protein Monkey Chow #5045) following testing and had access to water ad libitum. The animals were kept on a 12 h light/dark cycle and were given fresh fruits and vegetables daily in addition to their chow.

2.2.2 Drug Treatment

For in vivo administration in preclinical studies, basmisanil was formulated by the Roche Galenic Laboratories as a micro-suspension in a vehicle containing 1.25% HPMC (hydroxypropyl methylcellulose) and 0.1% DOSS (dioctyl sodium sulfosuccinate) unless specified otherwise below. Concentrations were chosen to achieve the desired doses by administering 5 mL kg^{-1} to rats and 2.5 mL kg^{-1} to NHPs via oral gavage. Pre-treatment times were selected for each species/test to correspond with maximum plasma concentrations of basmisanil, based on previously conducted pharmacokinetic experiments (for examples see Supporting Figure S1 and Tables S3 and S4).

2.2.3 Receptor occupancy in rats

To estimate in vivo $GABA_A$-α5 receptor occupancy in rats, [^{3}H]-Ro 15-4513 was employed as a radioligand using a similar experimental approach as described previously (Ballard et al., 2009). Female Sprague-Dawley rats were pretreated with vehicle or basmisanil at doses of 3, 10, 30 or 100 mg kg^{-1} p.o. (n = 4 per dose group, n = 2 for the 100 mg kg^{-1} group) and 45 min later received intravenously 0.1 mCi/kg of [^{3}H]-Ro 15-4513 (equivalent to a dose of 0.6 μg/kg).

For determination of non-specific binding of [^{3}H]-Ro 15-4513 one group of animals (n = 4) received the established $GABA_A$-α5 blocker L-655,708 (10 mg kg^{-1}) i.p. 30 min prior to radioligand injection (see (Atack et al., 2006). Rats were sacrificed by decapitation 15 min after administration of the radioligand, i.e., 60 min after administration of basmisanil. Brains and blood were collected from each animal. Brains were divided in two halves along their sagittal axis and frozen in dry ice. Blood plasma was used for the determination of the plasma concentrations of basmisanil. Half of the brain was used for autoradiography, as described earlier (Ballard et al., 2009). To obtain the specific binding (S), the radioactivity in the hippocampus of L-655,708-treated animals was subtracted from the radioactivity in the hippocampus of vehicle- and basmisanil-treated animals. The percentage of receptor occupancy (y) was calculated from:

$y = 100\ (1 - S_{basmisanil})\ /\ S_{vehicle}$.

Quantitative autoradiography signals in the hippocampus were plotted against individual plasma concentrations of basmisanil. The curve was fitted to the experimental results using the Hill equation (equation 1 with Hill coefficient D = 1).

2.2.4 Diazepam-induced spatial learning impairment in the Morris water maze

The Morris water maze is a test of spatial learning and memory which is dependent on hippocampal function (Morris, 1984). In this test, rats are challenged to find a hidden platform position when placed in a large pool filled with opaque water. Diazepam impairs spatial learning in naïve rats in this paradigm and it has been proposed that non-selective $GABA_A$ receptor PAMs may induce memory impairment by modulating hippocampal function (Ballard et al., 2005; McNaughton & Morris, 1987). The current study used a modified version of the standard acquisition protocol, in which pre-trained rats had to learn to locate a new platform position during six trials on the test day, as described previously (Ballard et al., 2009). Subjects were semi-randomly divided into treatment groups based on their performance on the last training day. A computer tracking system (HVS Image Ltd, UK) was used to analyse each rat's swim path on-line. Basmisanil (3 or 10 mg kg^{-1} p.o.) was administered to male Lister Hooded rats 30 min before the behavioural test (n = 10/dose group). Diazepam was prepared in 0.3% Tween 80 v/v 0.9% saline and was administered i.p. 30 min prior to testing. For estimating plasma levels at the time of testing, a separate cohort of rats was treated with basmisanil as described previously and were euthanized by decapitation either at 30 min (corresponding to start of testing) or 100 min (corresponding to end of testing) post-administration of the compound (n=4 per dose and time point). Plasma samples were collected and frozen at -80°C for later analysis.

2.2.5 Object retrieval task in cynomolgus macaques

In addition to rodents, the pro-cognitive properties of basmisanil were evaluated in NHPs in the object retrieval (or detour reaching) task. Object retrieval is a task of prefrontal cortical-mediated cognition in monkeys which involves planning and response inhibition, i.e., executive function (Rutten et al., 2008). Twelve cynomolgus macaques were presented with a clear acrylic box with one open side baited with a food treat, as described previously (Ballard et al., 2009; Rutten et al., 2008). The test is easy when the open side of the box is directed towards the subject and difficult when the open sides face other directions. In difficult trials, subjects obtained the treat on the first attempt approximately 50% of the time. Basmisanil (1, 3, 10, 30 mg kg^{-1}) was administered 2 h prior to testing (n =12/dose group; within-subjects design). Compound doses were administered in a pseudorandom order. Administration of dose and behavioural measurements were completed blind. Plasma samples were collected from the same three subjects at each dose group at 3 h post administration.

2.2.6 Pentylenetetrazole test

The potential for proconvulsant activity of basmisanil was evaluated in the pentylenetetrazole (PTZ) test in Wistar rats. In this assay, basmisanil was administered in combination with a sub-threshold dose of the convulsant PTZ (55 mg kg^{-1}, males; 70 mg kg^{-1}, females). PTZ was prepared in 0.9% saline and was administered s.c. in a volume of 1 mL kg^{-1}. The positive control FG7142, a non-selective $GABA_A$receptor NAM, was prepared in 0.3% Tween 80 v/v saline and was administered i.p. in a volume of 1 mL kg^{-1}. Immediately following PTZ administration, rats were placed into individual observation chambers (24 x 39 x 18 cm; Macrolon Type III cages) with sawdust coated floors and were observed for a 30 min period by an observer blind to the treatment (n = 8 rats per dose group; randomised). During this period the number of rats showing tonic convulsions was noted.

Basmisanil (3, 10, 30, 100 mg kg^{-1}) was administered to male rats 1 h prior to PTZ administration. In a separate experiment, basmisanil was administered to female rats 2 h (30, 100 mg kg^{-1}) or 3 h (300,

600 mg kg^{-1}) prior to PTZ administration. FG7142 was administered at 10 mg kg^{-1} 30 min prior to PTZ. Following tonic convulsions, rats were immediately euthanized by decapitation. All other rats were euthanized by decapitation at the end of the 30 min observation period. Plasma samples were collected and frozen at -80°C for analysis of drug content.

2.2.7 Social approach avoidance

In the social approach avoidance experiment, a F-344 Fischer rat can freely move between a non-social compartment (in particular, a hidden area) and a social compartment containing a large, unfamiliar stimulus rat (Sprague-Dawley) behind a perforated wall. The preference for the hidden area or for the social compartment reflects the anxiety state of the test animal. The test is suitable for assessing potential anxiogenic-like and anxiolytic-like effects of compounds (Nicolas & Prinssen, 2006; Rutten et al., 2008). Experiments on social approach avoidance were performed as described previously by (Nicolas & Prinssen, 2006) and (Ballard et al., 2009). A tracking system (Ethovision, Noldus, The Netherlands) was used to analyse each rat's pathway. Basmisanil was administered to male Fischer rats 1 h prior to testing at 3, 10, 30 and 100 mg kg^{-1} p.o. (n = 10 per treatment group; randomised). The positive control, Ro 19-4603, was suspended in 0.3% Tween 80 v/v 0.9% saline and administered at 3 mg kg^{-1} p.o. 30 min prior to testing. At the end of the test session rats were immediately euthanized by decapitation. Plasma samples were collected and frozen at -80 °C for analysis of drug content.

2.2.8 Bioanalysis

Basmisanil plasma concentrations were analysed from a column-switching HPLC method and turbo ion spray tandem quadrupole mass spectrometry (LC-MS/MS) detection with lower quantification limits of 1.0 ng mL^{-1}. The calibration range was from 1.0 ng mL^{-1} to 5000 ng mL^{-1}. After protein precipitation with ethanol, the sample solution was injected onto a Gemini C18 trapping column (2 x 10 mm; Phenomenex, Torrance, CA, USA) and polar endogenous compounds and salts were rinsed off. Analytical separation was performed on an Atlantis T3 column (2.1 x 50 mm) (Waters, Milford, MA, USA), using methanol/water containing 0.1% formic acid as mobile phase. A drug analogue was used as an internal standard.

2.3 Healthy Volunteer PET Receptor Occupancy Study

The study was approved by the North London Research Ethics Committee (REC) 3 (UK), reference 10/H0709/90, and permission to administer the radiotracer [^{11}C]-Ro 15-4513 was obtained from the Administration of Radioactive Substances Advisory Committee of the UK (Ref: 630/3764/28825).

2.3.1 Subjects

Subjects were screened and recruited at Hammersmith Medicine Research, and imaging assessments were conducted at the Imanova Centre for Imaging Sciences, London, UK. Nine healthy volunteers (7 males and 2 females, aged 21-39 years) were enrolled into the study meeting the protocol inclusion and exclusion criteria posted on the ClinicalTrials.gov database (clinicaltrials.gov identifier: NCT01667367).

2.3.2 Experimental procedures

Each subject received a baseline [^{11}C]-Ro 15-4513 PET scan (PET scan 1). After the baseline scan, each subject received a single oral dose of basmisanil, followed by a further PET scan (PET scan 2). PET scan 2 took place approximately 3-5 h post dose (in order to coincide with the anticipated time of maximum concentration of basmisanil). Subjects returned for a follow-up visit approximately 7 to 10 days after their last dose of study medication.

A range of doses of basmisanil were evaluated (20 mg (n=2); 40 mg (n=2); 80 mg (n=1); 160 mg (n=2); 1000 mg (n=2)), after the demonstration of safety and tolerability in a previous placebo-controlled, single ascending dose study completed in healthy male subjects (clinicaltrials.gov identifier: NCT01684891). Blood

sampling was performed at four different timepoints starting 30 min before the post dose PET scan. Quantification of plasma basmisanil was performed by liquid chromatography-tandem mass spectrometry, with the lower limit of quantification at 1.0 ng mL^{-1}.

2.3.3 Radiochemistry

[^{11}C]-Ro 15-4513 was prepared as described previously (Halldin et al., 1992).

2.3.4 Image acquisition

A structural T1-weighted magnetic resonance brain scan was acquired on a 3T MRI scanner (Siemens Tim Trio 3T; Siemens AG Medical Solutions, Erlangen, Germany). Data were acquired in the sagittal plane, using a 3D magnetization prepared rapid gradient echo (MP-RAGE) sequence with the following parameters: repetition time = 2300 ms, echo delay time = 2.98 ms, flip angle = 9°, isotropic voxels = 1.0 mm x 1.0 mm x 1.0 mm, 160 slices, total scanning time = 5 min, 03 sec. MRI scans were inspected by a neuroradiologist to exclude subjects with any clinically relevant brain abnormalities.

Dynamic PET scans were acquired on a Siemens Biograph 6 PET/computed tomography scanner with TruePoint gantry (Siemens AG Medical Solutions, Erlangen, Germany). Subjects were positioned in the tomograph after insertion of a venous cannula in an antecubital vein, a head-fixation device was used to minimize movement during data acquisition. A low-dose computed tomography scan was performed before each injection of the radioligand for attenuation and scatter correction. Dynamic emission data were collected continuously for 90 min (frame durations: 8 x 15 s, 3 x 60 s, 5 x 120 s, 5 x 300 s, 5 x 600 s) after intravenous bolus injection of [^{11}C]-Ro 15-4513 (range 264-314 MBq). Image data were reconstructed using Fourier rebinning and a 2D filtered discrete inverse Fourier transform algorithm with 5 mm isotropic Gaussian filter on a 128 x 128 matrix with 2.6 zoom giving 2 mm isotropic voxels. Corrections were applied for attenuation, randoms and scatter.

2.3.5 Image data analysis

Image processing

Image data were analysed using the MIAKAT software package (version 3.3.1). MIAKAT is implemented using Matlab (version R2008b; The Mathworks Inc., Natick, MA, USA), and makes use of FSL (version 4.1.9; FMRIB, Oxford, UK; (Jenkinson et al., 2005; Smith et al., 2004) functions for brain extraction and SPM5 (Wellcome Trust Centre for Neuroimaging, http://www.fil.ion.ucl.ac.uk/spm) for image segmentation and registration.

Each subject's structural MRI image underwent brain extraction, grey matter segmentation and co-registration to a standard reference space (MNI152, (Grabner et al., 2006). The MNI152 template brain image and associated atlas (CIC atlas (Tziortzi et al., 2011) was nonlinearly warped to the subject's MR image to enable automated definition of regions of interest (ROIs).

The following ROIs were considered: occipital lobe, parietal lobe, temporal lobe, amygdala, hippocampus, parahippocampal gyrus, insular cortex, anterior cingulate, dorsolateral frontal cortex, medial frontal cortex, orbitofrontal cortex, globus pallidus, caudate, accumbens, putamen, midbrain, medulla, pons and ventral cerebellum. ROIs were selected to provide broad coverage of the brain, and encompass a range of levels of $GABA_A$-α5 expression (Li, Szabo & Rosenberg, 2001) and [^{11}C]-Ro 15-4513 signal (based on previous literature [e.g. (Maeda et al., 2003)] and baseline data from this study).

Dynamic PET images were registered to each subject's MRI scan and corrected for motion using a frame-to-frame registration process with a normalized mutual information cost function. ROIs defined on the MRI images were applied to the dynamic PET data to derive regional time-activity curves (TACs), with activity concentrations expressed as standardized uptake values (SUV), given by (equation 2):

Equation 2: SUV = Act/(IA/BW)

where Act is the measured radioactivity concentration (kBq/ml), IA is the injected radioactivity (MBq) and BW is the subject's bodyweight (kg).

Kinetic modelling

Tissue time activity curves were analysed using the simplified reference tissue model (SRTM; (Lammertsma & Hume, 1996), with a basis pursuit implementation of the SRTM (Gunn et al., 1997), to directly estimate the binding potential (BP_{ND}) in all target regions. Though the pons has the lowest [^{11}C]-Ro 15-4513 signal, it is thought to be poorly representative of target regions in terms of nonspecific binding. Therefore, the time-activity curve derived from the cerebellum was used as an input for SRTM analysis. Methods of quantification of [^{11}C]-Ro 15-4513 have been previously reported (Myers et al., 2017) test-rested variability for [^{11}C]-Ro 15-4513 has also been reported (McGinnity et al., 2017).

Occupancy in scan 2 was estimated as a fractional reduction in the relevant baseline BP_{ND} (see equation 3).

Equation 3: $Occ = (BP_{ND}{}^{Baseline} - BP_{ND}{}^{Basmisanil})/BP_{ND}{}^{Baseline}$

2.4 Healthy Volunteer EEG

2.4.1 Subjects

EEG was assessed during a drug-drug interaction (DDI) study of basmisanil with the non-selective $GABA_A$ PAM, midazolam. Twelve healthy volunteers (9 males and 3 females, aged 25-57 years) were screened and recruited at Covance Clinical Research Unit, Ltd, Leeds, UK (clinicaltrials.gov identifier: NCT02254759).

2.4.2 Experimental Procedure

Participants and experimental task. Resting state EEG (4 min eyes open, 4 min eyes closed) was recorded at 4 days 1 h and 4 h after dosing at morning (similar time at baseline day). Assessments days: baseline, midazolam (5 mg, oral administration), 14 days of basmisanil treatment (240 mg twice daily, oral administration, recording following morning dose at day 14), and after 16 days of basmisanil treatment (240 mg twice daily, oral administration, recording following morning dose at day 16) plus midazolam (5 mg, oral administration). The EEG technician kept the subject alert (vigilance controlled resting state condition). As soon as drowsiness patterns appeared (slow rolling eye movements, attenuated alpha rhythm replaced by low amplitude), the subject was aroused by auditory stimuli (tapping or clicking).

Blood sampling. Blood samples for basmisanil were collected on Day 18 of the study, at scheduled times up to 10 h after the administration of midazolam and up to 12 h after the administration of basmisanil. Concentration data collected at the time corresponding to the maximum plasma concentration for basmisanil (4 h post-dose) were used for the purpose of the pharmacokinetic/pharmacodynamic analysis.

EEG recording. EEG was recorded from 19 Ag/AgCl electrodes arranged according to the 10/20 system and mounted in an elastic cap. EOG was recorded simultaneously from five electrodes. Data were acquired at sampling rate of 256 Hz (alpha trace digitalEEG EPV-32, Neuro Medical, Arnheim, Netherlands; high-pass: 0.16 Hz; low-pass filter: 70 Hz; line-noise notch filter at 50 Hz; recording reference POz). Impedances were kept below 20 k.

Preprocessing. All pre-processing was performed blinded to the treatment. Eyes open and eyes closed resting state data sections were extracted, high-pass filtered (0.5 Hz, FIR filter, n = 2 x sampling rate), and line-noise notch-filtered (Butterworth filter 49 – 51 Hz, order 4). Data sections confounded by large technical artifacts (e.g. large-amplitude transients) or prominent physiological artifacts (e.g. strong muscle activity) where identified by visual inspection and excluded from further processing. Then independent component analysis was applied to all of each subject's recordings from a day to remove remaining artifacts (artifactual ICs rejected: muscle, ECG, eye movements and blinks, technical artifacts, number of rejected ICs: 4.9 ± 1.94, mean ± SD, range: 1–9). Finally, the data was re-referenced to average reference. Pre-processing resulted in 221 ± 26.7 s (mean ± SD, range: 114–240 s) of data per subject and condition for analysis. Overall the

data quality was suitable for the planned analyses judged by fraction rejected as artifacts and qualitative impression of EEG traces.

*Individual alpha peak frequency***.** Individual alpha peak frequency was defined as the maximum in the frequency range of 7–12 Hz of the power spectrum extracted from eyes closed resting state data at baseline (FFT applied to artifact free data in a 1 s sliding window, 3/4 overlap, zero-padded to 25 s). The existence of an alpha peak was confirmed in all 12 subjects visually. As would be expected, alpha peak frequencies (9.3 ± 0.87 Hz, mean ± SD, range: 8.2– 0.7 Hz) varied substantially across subjects.

Power spectral estimates. Power spectral estimates were derived for logarithmically scaled frequencies with a logarithmic frequency smoothing using Morlet Wavelets with a spectral smoothing of 1/2 octave ($f/\sigma f = 5.83$). Frequencies were spaced logarithmically according to the exponentiation of the base 2 with exponents ranging from 1 (2 Hz) to 6 (64 Hz) in steps of 1/8. Spectral estimates were derived in successive 3/4-overlapping temporal windows. This frequency transform accounts for the logarithmic nature of electrophysiological data (Buzsaki & Draguhn, 2004). The analysis accounted for intra-individual differences in alpha peak frequency by individually adapting frequencies (individual shifts of the center frequencies in log-space) to align all alpha peaks to the mean across subjects (9.3 Hz). This allowed us to pin-point possible effects relative to the alpha peak frequency. Power values where scaled to have units $V^2/\log_2(Hz)$. For analyses of "relative power" the power was normalized to 1 across the frequency range analysed.

2.5 Data and Statistical Analysis

The data and statistical analysis comply with the recommendations on experimental design and analysis in pharmacology (Curtis et al., 2018). Data are presented as mean ± SEM, unless stated otherwise. The accepted level of significance for all experiments is $P < 0.05$.

In vitro studies

Binding affinity: The relation between specific binding and modulator concentration was fitted by the equation

$y = A + (B - A) / [1 + (C / x)^D]$ (equation 1)

with y = % specific binding, A = minimum y, B = maximum y, C = IC_{50}, D = slope (Hill coefficient) and x = concentration of basmisanil. From the estimated value of IC_{50} we calculated the affinity constant (K_i) using the Cheng-Prusoff equation, $K_i = IC_{50} / (1+ (L / K_d)$, where L is the concentration (1 nM) and K_d is the affinity constant of the radiolabel, [^{3}H]-flumazenil. The previously determined values of K_d are 1.14 nM, 1.59 nM, 1.75 nM and 0.46 nM for α1, α2, α3 and α5 containing receptors, respectively. For Ro 15-4513, the concentration was also 1 nM and the Kd values were 1.01 nM and 1.83 nM for α4 and α6 containing receptors, respectively.

Function of cloned $GABA_A$ receptors: To determine concentration-response relationships, we calculated for each oocyte the ratio of the GABA-induced currents recorded in the presence and absence of the test compound to estimate modulation of the GABA response induced by the compound. For obtaining concentration-response curves, the data was fitted by equation 1 with A = 0.

Receptor occupancy. The relation between the free plasma concentration of basmisanil (x) and the receptor occupancy (y) in hippocampal slices was fitted by equation 1 with a fixed Hill coefficient (D = 1).

In vivo studies

Morris water maze in rats. Latency, pathlength and swim speed (Supporting Figure S2) were analysed with a one-factor ANOVA. For the probe trial, to determine whether each treatment group had learned the spatial position of the platform, within-subjects ANOVA was used to compare percent time spent in the platform quadrant with the left, right and opposite quadrants. All significant cases were followed by a post

hoc Newman-Keuls test. In addition, a comparison between vehicle treated and diazepam-treated rats on the percent time spent in the platform quadrant was analysed using an unpaired t-test.

Object retrieval task in cynomolgus macaques. Data were analysed using a one-way repeated measures ANOVA followed, in significant cases, by a post hoc Dunnett's test.

Proconvulsant activity. The percent of rats in each dose group showing tonic convulsions was compared to the control group by the Pearson Chi-Square test.

Social approach avoidance tests . All basmisanil dose groups were compared to the corresponding control group using a one-way ANOVA followed, in significant cases, by Dunnett's post hoc test. The effects of the reference compound, Ro 19-4603, was compared with vehicle using an unpaired t-test.

Healthy Volunteer PET: Pharmacokinetic-Target Occupancy Analysis

The pharmacokinetic/pharmacodynamic population for $GABA_A$-α5 receptor occupancy consisted of data from 9 subjects. A simple Emax model was found to describe the data adequately. This model was fitted to the whole data set using GraphPad Prism, version 5.03 (GraphPad Software, San Diego CA) to obtain estimates of EC_{50}:

$E = E_{max}$* [basmisanil]/ (EC_{50} + [basmisanil]).

Healthy Volunteer EEG

Student's t-tests were used for single comparisons and to derive confidence intervals. To test for differences in spectral power across frequencies cluster randomization tests were employed (Nichols & Holmes, 2002). To this end the condition labels for the contrast of interest (e.g. baseline and drug) were randomized (n=10,000), t-test were performed for each frequency (two-tailed), then clusters (contiguous frequency ranges with values below the threshold) were identified, and the size of the largest cluster across the entire frequency space from each randomization was used to generate a Null-hypothesis distribution. Cluster-randomization statistics accounts for multiple-comparison across all frequencies as well as positive and negative changes (two-tailed) in a data-adaptive manner.

We derived individual estimates of peak frequencies of pharmacological effects using pseudo-values (Miller, 1974) in order to (a) estimate the standard error of the mean of the peak frequency of effects and (b) to compare peak frequencies of effects induced by midazolam and basmisanil.

To investigate possible differences in the spatial topography of drug effects (reflective on the spatial localization of the underlying neuronal populations), we compared the average mutual correlation between all subjects' topographies for basmisanil and the average mutual correlation between all subjects' topographies induced by midazolam to the correlation of topographies between drugs. Significance was assessed by means of a randomization test.

All analyses were performed in Matlab with custom scripts and the Fieldtrip toolbox to generate topographic plots.

2.5 Materials

Basmisanil was synthesized at F. Hoffmann-La Roche AG (Basel, Switzerland) as described in WO2013/057123 A1 (Dott et al., 2013). $GABA_A$ receptor modulators, i.e., diazepam, midazolam, flumazenil (Ro 15-1788), Ro 19-4603, L-655,708, FG7142, pentylenetetrazole (PTZ) and the radioligands [^{3}H]-flumazenil ([^{3}H]-Ro 15-1788) and [^{3}H]-Ro 15-4513 were also synthesized at F.Hoffmann-La Roche AG.

For the in vitro experiments all compounds were obtained from Fluka, unless otherwise indicated. GABA, isoguvacine and β-CCM were purchased from Sigma-Aldrich.

For the healthy volunteer studies, basmisanil was provided as an uncoated, immediate-release tablet formulation exhibiting four different dose strengths (0.5, 5, 40, and 250 mg) as described by (Stillhart et al., 2017).

3 Results

3.1 Βασμισανιλ εξηιβιτς ηιγη αφφινιτψ ανδ σελεςτιιτψ φορ ηυμαν ΓΑΒΑ$_A$-α5 ρεςεπτορς

As shown in Figure 2A and Table 1 basmisanil bound with high affinity and more than 90-fold selectivity to membranes containing α5β3γ2 receptors compared to HEK293 cells expressing the human GABA$_A$ receptor subunits α1, α2 or α3 in conjunction with the β3 and γ2 subunits. Comparable affinity and selectivity were found for rat GABA$_A$ receptors expressed in HEK293 cells (data not shown). Basmisanil binding to human α5β3γ2 showed > 600-fold selectivity compared to human α4β3γ2 and α6β3γ2, i.e., no binding at 3160 nM (data not shown).

Further studies were conducted by Eurofins CEREP to assess the binding of basmisanil (10 μM) to 78 other receptors, transporters and ion channels. (Supporting Table S2). The compound showed at least 2,000-fold selectivity for the GABA$_A$ α5β3γ2 subtype over all the targets tested with exception of the sigma receptor, where it produced 58% displacement of the label, [^{3}H]-DTG.

3.2 Βασμισανιλ εξηιβιτς φυνςτιοναλ σελεςτιιτψ φορ ηυμαν ΓΑΒΑ$_A$-α5 ρεςεπτορς

Basmisanil showed a highly selective inhibition of GABA$_A$-α5 (Figure 2B). Basmisanil reduced the GABA-evoked current by up to 39% (Table 1), which is slightly less effective than the unselective NAM, β-CCM (52%, data not shown). The weak effects of basmisanil on receptors containing other α subunits was not due to a malfunction of the receptors since β-CCM produced the expected inhibition, i.e., reduced the GABA-evoked current by approximately 50% (data not shown).

We also looked for the functional competition between basmisanil and flumazenil, a non-selective weak PAM at cloned GABA$_A$receptors (Figure 2C and D). Flumazenil concentration-dependently (30 and 1000 nM) enhanced the GABA-induced current in α5-expressing oocytes up to 28%. This effect is much weaker than that of midazolam, a full PAM, causing 145±9% increase at 1000 nM (n=12, not shown). Basmisanil administered alone, decreased the GABA-induced current and this effect was blocked by co-treatment with flumazenil (Figure 2D).

3.3 Δοσε-δεπενδεντ ΓΑΒΑ$_A$-α5 ρεςεπτορ οςςυπανςψ βψ βασμισανιλ ιν ρατ βραιν

Autoradiographical analysis after intravenous injection of the radioligand revealed a binding pattern that is in good agreement with the known distribution of GABA$_A$-α5 receptors (Fritschy et al., 1997; Pirker et al., 2000). Strongest binding under baseline conditions was observed in brain regions known to contain high densities of GABA$_A$-α5 receptors, such as the hippocampus and the frontal cortex, whereas regions containing less GABA$_A$-α5 such as the striatum and the cerebellum showed lower densities of [^{3}H]-Ro 15-4513 binding (Figure 3A). To visualize non-specific binding of the radioligand, rats were pretreated with the α5-selective ligand L-655,708 (10 mg kg^{-1} i.p.) (Figure 3A; (Quirk et al., 1996) Densities of specific [^{3}H]-Ro 15-4513 binding sites in vehicle-treated animals were 304 ± 15, 192 ± 15, 25 ± 5 and 38 ± 4 fmol mg^{-1} protein in the hippocampus, frontal cortex, striatum and cerebellum, respectively.

Pre-treatment with basmisanil (3-100 mg kg^{-1} p.o.) decreased the binding of [^{3}H]-Ro 15-4513 in a dose-dependent manner (Figure 3A). The highest dose (100 mg kg^{-1}) reduced specific binding in the hippocampus by 70 +- 6%. Binding data were further analysed by plotting specific receptor occupancy against the plasma concentration of basmisanil of each individual (Figure 3B). Fitting the data by the Hill equation (i.e., equation 1) resulted in a maximal occupancy of 77 +- 5% and plasma level of 544 +- 125 ng mL^{-1} (228 +- 52 nM free plasma concentration) for producing half-maximal receptor occupancy (EC_{50}).

3.4 Basmisanil attenuated diazepam-induced spatial learning impairment in the Morris water maze test in rats

Diazepam significantly increased the latency and pathlength to find the platform position and induced a small but significant increase in swim speed (Supporting Figure S2). Basmisanil did not significantly reduce the diazepam-induced increase in latency and pathlength and had no effect on swim speed (Supporting Figure S2).

The platform was removed before the seventh trial. The vehicle group demonstrated spatial learning of the platform position, as indicated by the significant increase in percent time spent in the platform quadrant compared to left, right and opposite quadrants (Figure 4A). Diazepam significantly disrupted learning of the new platform position since subjects spent an equivalent amount of time in each quadrant during the probe trial. Moreover, there was a significant difference between vehicle and diazepam-treated groups in the percent time spent in the platform quadrant. Basmisanil at 10 mg kg^{-1} p.o. significantly attenuated the diazepam-induced deficit as revealed by an increase in percent time spent in the previous platform quadrant compared to left, right and opposite quadrants (Figure 4A).

Plasma concentrations of basmisanil as determined in parallel dose groups were dose- and time-dependent (Supporting Table S5) and reached a maximal level of 903 +- 13 ng mL^{-1} (379 +- 5 nM free plasma) 30 min after the administration of basmisanil at 10 mg kg^{-1} (Figure 5). Using Figure 3B and assuming that the asymptotic maximum of the curve actually corresponds to 100% occupancy of $GABA_A$-α5 receptors, occupancy during the water maze experiment was estimated to be between 45 and 65%.

3.5 Basmisanil improved percent correct in the object retrieval task in adult cynomolgus macaques

Basmisanil significantly improved the percentage of correct first reaches during difficult trials of the object retrieval task at the 3 and 10 mg kg^{-1} doses (Figure 4B). Basmisanil exhibited an inverted U-shaped dose response in this paradigm with the 1 and 30 mg kg^{-1} doses producing no marked improvement on performance. The total plasma exposure increased with dose (Supporting Table S6). Active free plasma concentrations were 156 and 345 nM (Figure 5), which corresponded to about 30 and 50% estimated receptor occupancy.

3.6 Lack of proconvulsant activity of basmisanil at therapeutically relevant concentrations in the PTZ test

Single doses of basmisanil up to 100 mg kg^{-1} in male rats (total plasma concentration of 3864 ng mL^{-1}; 1622 nM free plasma concentration) and 30 mg kg^{-1} in female rats, (total plasma concentration of 5840 ng mL^{-1}; 2452 nM free plasma concentration; Figure 5) did not exert proconvulsant activity in the PTZ test (Table 2). The receptor occupancies estimated at these plasma concentrations are approximately 60-70% for α5 receptors, which are the maximum observed in the in vivo binding experiments described above. In female rats at a dose of 100 mg kg^{-1} (total plasma concentration of 12100 ng mL^{-1}; 5079 nM free plasma concentration; Figure 5) five out of eight rats exhibited tonic convulsions following administration of a sub-threshold dose of PTZ. The two higher doses produced identical effects (Table 2) and had similar plasma concentrations to 100 mg kg^{-1} (Supporting Tables S7 and S8). The positive control, FG7142, significantly increased the number of rats showing tonic convulsions, as expected (Table 2).

3.7 Basmisanil did not have an anxiogenic effect in the social approach avoidance test in rats

Basmisanil did not significantly reduce the time spent in the social compartment or increase the time spent in the hidden area at any dose up to 100 mg kg^{-1} (Table 3). Plasma concentrations between 414 to 7288 ng mL^{-1} (174 to 3059 nM free plasma concentrations; Figure 5) were found (Supporting Table S9) with estimated receptor occupancies of 50 to 77%. As expected (Nicolas & Prinssen, 2006), the non-selective $GABA_A$ NAM used as a positive control, Ro 19-4603, significantly decreased the time in the social compartment and increased the time in the hidden area (Table 3).

3.8 Δοσε-δεπενδεντ ΓΑΒΑ$_A$-α5 ρεςεπτορ οςςυπανςψ βψ βασμισανιλ ιν ηυμαν βραιν οφ ηεαλτηψ ολυντεερς

The degree of receptor occupancy by basmisanil was determined in healthy volunteers using PET and [^{11}C]-Ro 15-4513. PET images of the brain at baseline displayed a spatially structured signal consistent with previously published [^{11}C]-Ro 15-4513 PET data and the known distribution of $GABA_A$-α5 subunit-containing receptors, with the highest signal in the hippocampus, nucleus accumbens, amygdala and cortical regions (Myers et al., 2017); Figure 6A). Following administration of basmisanil, heterogeneity in both summed PET images and tissue time activity curves was reduced relative to baseline scans, indicating blocking of [^{11}C]-Ro 15-4513 $GABA_A$-α5 receptor binding by basmisanil. A dose-dependent decrease in [^{11}C]-Ro 15-4513 binding in all regions was observed after administration of basmisanil. The calculated $GABA_A$-α5 receptor occupancy at the highest dose of 1000 mg basmisanil reached 94% in the hippocampus (Supporting Table S11). The relationship between receptor occupancy and plasma concentrations can be described by a simple Emax model, suggesting a direct relationship i.e., no significant delay in receptor occupancy compared to plasma concentration, with an EC_{50} of approximately 541 ng mL^{-1} total plasma concentration corresponding to 67 nM free plasma concentration (Figure 6B).

3.9 Electrophysiological signature of basmisanil in healthy volunteers

Twelve healthy volunteers underwent resting state EEG assessments at baseline, after an acute dose of midazolam, and after 14 days of sub-chronic treatment with basmisanil. Treatment with basmisanil (240 mg twice daily) led to high occupancy of $GABA_A$-α5 receptors of > 90% (plasma exposure at 1 h 3284 ± 887.9 ng mL^{-1} and 4 h 4030 ± 842.3 ng mL^{-1}; receptor occupancy after 1 h 92 ± 3% and after 4 h 94 ± 1.5%; exposure and occupancy ranges during EEG assessments are depicted in Figure 6B).

Basmisanil significantly increased relative power in the theta- to low alpha frequency range (6.2 – 8.7 Hz; Figure 7A) by 19.1 ± 3.3% compared to pre-treatment baseline. The peak frequency of the effect was 7.3 ± 0.4 Hz, which was below the mean alpha peak frequency of 9.3 Hz. Furthermore, basmisanil significantly decreased relative power in the beta- to low gamma frequency range (13.5–38.0 Hz; peak frequency of 34.9 ± 3.13 Hz) by 18.9 ± 4.24% compared to the pre-treatment baseline. We performed a series of additional analyses to further investigate the nature of these effects. First, we confirmed a similar spectral pattern for absolute power (Supporting Figure 5D), while only the low-frequency peak survived multiple-comparison correction. Second, the above analyses combined 1 h and 4 h post dose assessments as well as eyes open and eyes closed conditions. Analysing each of the four conditions separately suggested that the spectral signature is similar across all four conditions (Supporting Figure 5C).

The spectral pattern induced by basmisanil was qualitatively opposite to that of midazolam, characterized by a decrease of relative power at low frequencies in the high theta to low alpha bands (8.2 ± 4.12 Hz, -14.4 ± 3.73%) and increases at higher frequencies in the beta band (18.4 ± 6.06 Hz, 32.2 ± 7.04%) (Figure 7A, gray band; Supporting Figure 5E). However, the peak frequency of the beta to gamma band effect was significantly higher for basmisanil compared to midazolam (no significant difference for low-frequency effect). Furthermore, the spatial topography of the beta to gamma band effects significantly differed for basmisanil

and midazolam likely reflecting the difference in expression pattern of targeted receptors (within/between drug cross-subject correlation r = 0.128/0.003; Figure 7B, Supporting Figure 5F).

3.10 Safety in Healthy Human Volunteers in the PET and EEG studies

Basmisanil was safe and well tolerated in the healthy subjects evaluated in the PET and EEG studies. There were no severe adverse events, discontinuations or temporary discontinuations due to adverse events, in any cohort.

Discussion and Conclusions

Preclinical Profile of Basmisanil

Basmisanil bound to the BZD binding site of recombinant human $GABA_A$-α5 with 5 nM affinity and more than 90-fold selectivity versus α1, α2, and α3 subunit-containing receptors, as demonstrated by our flumazenil competition binding assays. Basmisanil also showed functional selectivity, since it inhibited GABA-induced current in cells expressing $GABA_A$-α5 yet had little or no effect at the other receptor subtypes. By combining the highly selective preference in affinity and efficacy at $GABA_A$-α5 versus $GABA_A$ α1, α2, and α3 subunit-containing receptors, basmisanil represents the most selective and potent $GABA_A$-α5 NAM in clinical development described so far.

Our in-vivo binding experiments using ^{3}H-Ro 15-4513 as a label for $GABA_A$-α5 receptors resulted in a binding curve for basmisanil approaching a maximum at 77%. Thus, 23% of the^{3}H-Ro 15-4513 binding sites could not be occupied by basmisanil. This can be explained by the limited selectivity of the radiolabel and the relative abundance of α1- and α2-containing receptors. For Ro 15-4513 published affinity ratios α1/α5 or α2/α5 range between 11 and 15 (Casula et al., 2001; Hadingham et al., 1993; Quirk et al., 1996). In the hippocampus, α5-containing receptors were found to account for 16-26% of all $GABA_A$ receptors (McKernan et al., 1991; Sur et al., 1999). From these values and equation 6 (see Supporting Information: [^{3}H]-Ro 15-4513), 17-33% of [^{3}H]-Ro 15-4513 is expected to bind to α1- and α2-containing receptors, which is in good agreement with the basmisanil in-vivo binding curve (Figure 3). In similar experiments with our previous α5-selective NAM, RO4938581, up to 90% of the binding sites of^{3}H-Ro 15-4513 in the hippocampus were occupied by the compound (Ballard et al., 2009) The apparent higher receptor occupancy of RO4938581 compared to basmisanil may be due to the lower binding selectivity of RO4938581, which was about 40-fold versus α1- and α2-containing receptors (Ballard et al., 2009). In the present study, basmisanil was 68- and 129-fold selective versus α2- and α1-containing receptors respectively, which suggests why the maximal receptor occupancy achieved with this compound is 77%. Overall, basmisanil demonstrated dose-dependent target engagement in vivo in rats.

In the spatial learning and memory test, acute administration of basmisanil at 10 mg kg^{-1} (estimated receptor occupancy between 45-65%) significantly attenuated the diazepam-induced impairment. Reversal of diazepam impairment has been proposed to be mediated via reduced activation of $GABA_A$-α5 receptors (Ballard et al., 2009). In NHPs basmisanil improved performance in the object retrieval task at estimated $GABA_A$-α5 receptor occupancy between 30-50%, which is similar to the rodent study. However, there was an inverted U-curve which was not observed in the rodent study. The lack of effect of higher doses was not due to lack of exposure, since plasma concentrations increased dose-dependently. A possible explanation may be that in the rodent study basmisanil was assessed in a pharmacologically-impaired model and so had to reverse an existing cognitive deficit. In non-impaired rodents $GABA_A$-α5 NAMs, including basmisanil and RO4938581, have not shown enhancement of cognitive performance (data not shown). In contrast the NHPs were healthy, unimpaired adults which performed at lower accuracy due to task difficulty. In this healthy condition, strongly decreasing $GABA_A$-α5 activity may not be beneficial for cognition. In summary, basmisanil exhibited cognition enhancing properties in pharmacologically-induced spatial learning impairment in rats and in an executive function task in NHPs.

Importantly, at plasma concentrations shown to improve cognition with estimated receptor occupancy of 30-65%, basmisanil lacked anxiogenic and proconvulsant potential, underlining the critical importance of subtype selectivity in binding affinity and functional efficacy (Figure 5). Moreover, sensorimotor gating was not affected by basmisanil at receptor occupancy of 40-50% (Supporting Figure S3 and Table S10); although higher doses were not tested. In the PTZ test, basmisanil exhibited proconvulsant activity only at supra-therapeutic high plasma exposure, which may be due to binding at other α subtypes. In contrast, preclinical GLP toxicology and safety pharmacology studies have shown no convulsions and no EEG alterations following daily oral administration of basmisanil at supra-therapeutic plasma exposures for up to 26 weeks in rats and 39 weeks in dogs (see Supporting Figure S4). The discrepancy between the PTZ test and the GLP toxicology studies may be related to synergistic activity through PTZ in the GABAergic system. It has been suggested that application of the PTZ test to assess the proconvulsant activity of drugs that antagonize GABA either directly or indirectly may lead to false positive conclusions and over-estimate the pro-convulsive risk of the molecule in question (Loscher, 2009).

Clinical Profile of Basmisanil in Healthy Volunteers

To confirm absence of pro-convulsive risk in humans at therapeutic exposures, EEG monitoring was included in Phase I studies covering high plasma exposures of basmisanil (see Supporting Clinical Information). In the MAD study, doses of 80, 160, 370 and 1000 mg were administered twice daily resulting in a mean maximum plasma concentration of 2120 (27% coefficient of variation), 4110 (31.3%), 6040 (26.5%) and 8520 (32.2%) ng mL^{-1}, respectively (six healthy volunteers per dose). In an itraconazole DDI study, plasma levels of basmisanil as a sensitive CYP3A substrate raised to 14500 ± 1810 ng mL^{-1} (n = 12 healthy volunteers). The maximum plasma concentration values observed in the MAD and DDI study exceeded those needed for full receptor occupancy at trough by approximately six-fold. EEG readings did not reveal signals of pro-convulsive effects, such as epileptiform abnormalities, mirroring the high receptor selectivity shown in vitro and in line with the lack of clinical signs and convulsion symptoms in GLP toxicology studies in dogs at exposures up to 4590 ng mL^{-1}.

PET imaging data, obtained in vivo in healthy human volunteers, indicates that basmisanil enters the brain and blocks the binding of the $GABA_A$-α5 preferring ligand [^{11}C]-Ro 15-4513 in a dose dependent manner. The relationship between receptor occupancy and basmisanil plasma concentration can be described by a simple Emax model suggesting a direct relationship, i.e., no significant delay in receptor occupancy compared to plasma concentration, with an EC_{50} of approximately 541 ng mL^{-1} total plasma concentration, corresponding to 67 nM free plasma concentration. Understanding the drug concentration-occupancy relationship will allow dosing regimens for future clinical trials to be selected in such a way as to adequately cover a specific target occupancy.

EEG assessment of basmisanil in healthy volunteers, revealed that negative modulation of $GABA_A$-α5 receptors leads to an increase in lower frequency EEG power (theta to alpha frequency range) and a decrease in higher frequency EEG power (beta to gamma frequency range). These results demonstrate that basmisanil has an effect on brain function and suggest EEG as a pharmacodynamic readout for future clinical studies.

Non-selective $GABA_A$ PAMs, i.e. BZDs, are known to induce a characteristic EEG signature with an increase in beta-band activity which is an established pharmacodynamic marker, and a decrease of activity at lower frequencies (Friedman et al., 1992; Malizia et al., 1996; Visser et al., 2003). Non-selective $GABA_A$ NAMs (e.g. DMCM, Ro 19-4603) have been shown to reduce beta-band activity in rodents (Visser et al., 2003). Furthermore, genetic links between beta-band activity and SNPs in $GABA_A$ receptor genes (Porjesz et al., 2002; Smit et al., 2018) and for rare genetic conditions involving CNVs (Dup15q syndrome, Angelman syndrome) including $GABA_A$ receptor genes (Frohlich et al., 2019a; Frohlich et al., 2019b) have been reported. $GABA_A$ receptor-related changes in beta-band activity are thought to reflect modulation of recurrent excitatory-inhibitory feedback loops in cortical tissue (Traub et al., 1999; Whittington et al., 2000), but are not understood in detail. Thus, the EEG effects of basmisanil are well aligned in terms of frequency bands affected and directionality of the change with prior work on $GABA_A$ receptor modulators. Future studies should investigate how modulation of the different BZD-sensitive receptor subtypes, by subtype

selective ligands, can lead to qualitatively similar changes in the large-scale oscillatory activity.

The EEG study has limitations, which should be considered. The number of subjects was low (n=12), there was no placebo condition, and only a clinical EEG with 19 electrodes was used, which makes it difficult to clean high-frequency artifacts to study gamma band activity (Hipp & Siegel, 2013). Only a high dose (>90% receptor occupancy) in sub-acute treatment regime (following 14 days of basmisanil dosing) was tested. Furthermore, the effect in the beta frequency range was not significant for absolute power when correcting for multiple testing across frequencies. Future studies need to confirm these findings, identify the pharmacokinetic/pharmacodynamic relationship and understand if the findings also generalize to acute and long-term treatment with basmisanil.

Summary and Conclusions

Our preclinical studies showed that the in vitro pharmacological profile of basmisanil translates into efficacy in cognition paradigms together with an adequate safety profile at estimated $GABA_A$-α5 receptor occupancy of around 30-65%. Our clinical studies demonstrated direct target engagement using PET and our first EEG study provided evidence for functional target engagement of basmisanil in humans. Further studies are required to determine whether this would be a useful pharmacodynamic biomarker for $GABA_A$-α5 receptor activity.

References

Atack JR (2010). Preclinical and clinical pharmacology of the $GABA_A$ receptor α5 subtype-selective inverse agonist α5IA. Pharmacology & therapeutics 125**:** 11-26.

Atack JR, Bayley PJ, Seabrook GR, Wafford KA, McKernan RM, & Dawson GR (2006). L-655,708 enhances cognition in rats but is not proconvulsant at a dose selective for α5-containing $GABA_A$ receptors. Neuropharmacology 51**:** 1023-1029.

Atack JR, Maubach KA, Wafford KA, O'Connor D, Rodrigues AD, Evans DC*, et al.* (2009). In vitro and in vivo properties of 3-tert-butyl-7-(5-methylisoxazol-3-yl)-2-(1-methyl-1H-1,2,4-triazol-5-ylmethoxy)-pyrazolo[1,5-d]-[1,2,4]triazine (MRK-016), a $GABA_A$ receptor α5 subtype-selective inverse agonist. J Pharmacol Exp Ther 331**:** 470-484.

Ballard TM, Knoflach F, Prinssen E, Borroni E, Vivian JA, Basile J*, et al.* (2009). RO4938581, a novel cognitive enhancer acting at $GABA_A$ α5 subunit-containing receptors. Psychopharmacology 202**:** 207-223.

Ballard TM, Woolley ML, Prinssen E, Huwyler J, Porter R, & Spooren W (2005). The effect of the mGlu5 receptor antagonist MPEP in rodent tests of anxiety and cognition: a comparison. Psychopharmacology (Berl) 179**:** 218-229.

Braudeau J, Delatour B, Duchon A, Pereira PL, Dauphinot L, de Chaumont F*, et al.* (2011). Specific targeting of the GABA-A receptor α5 subtype by a selective inverse agonist restores cognitive deficits in Down syndrome mice. Journal of psychopharmacology (Oxford, England) 25**:** 1030-1042.

Bundgaard C, Badolo L, & Redrobe JP (2013). RO4938581, a $GABA_A$α5 modulator, displays strong CYP1A2 autoinduction properties in rats. Biochem Pharmacol 85**:**1363-1369.

Buzsaki G, & Draguhn A (2004). Neuronal oscillations in cortical networks. Science 304**:**1926-1929.

Casula MA, Bromidge FA, Pillai GV, Wingrove PB, Martin K, Maubach K*, et al.* (2001). Identification of amino acid residues responsible for the α5 subunit binding selectivity of L-655,708, a benzodiazepine binding site ligand at the $GABA_A$ receptor. J Neurochem 77**:** 445-451.

Chen ZW, Chang CS, Leil TA, Olcese R, & Olsen RW (2005). $GABA_A$ receptor-associated protein regulates $GABA_A$ receptor cell-surface number in Xenopus laevis oocytes. Molecular pharmacology 68**:** 152-159.

Clarkson AN, Huang BS, Macisaac SE, Mody I, & Carmichael ST (2010). Reducing excessive GABA-mediated tonic inhibition promotes functional recovery after stroke. Nature 468**:** 305-309.

Curtis MJ, Alexander S, Cirino G, Docherty JR, George CH, Giembycz MA*, et al.* (2018). Experimental design and analysis and their reporting II: updated and simplified guidance for authors and peer reviewers. Br J Pharmacol 175**:**987-993.

Dawson GR, Maubach KA, Collinson N, Cobain M, Everitt BJ, MacLeod AM*, et al.* (2006). An inverse agonist selective for α5 subunit-containing $GABA_A$receptors enhances cognition. J Pharmacol Exp Ther 316**:**1335-1345.

Dorow R, Horowski R, Paschelke G, & Amin M (1983). Severe anxiety induced by FG 7142, a β-carboline ligand for benzodiazepine receptors. Lancet 2**:** 98-99.

Dott P, Hanlon SP, Hildbrand S, Iding H, Thomas A, & Waldmeier P (2013). inventors, F. Hoffmann-La Roche AG, assignee. Process for the preparation of isoxazolyl-methoxy-nicotinic acids. International Patent WO 2013/05712 A1. 2013 April 25.

Fischell J, Van Dyke AM, Kvarta MD, LeGates TA, & Thompson SM (2015). Rapid Antidepressant Action and Restoration of Excitatory Synaptic Strength After Chronic Stress by Negative Modulators of α5-Containing $GABA_A$ Receptors. Neuropsychopharmacology 40**:** 2499-2509.

Friedman H, Greenblatt DJ, Peters GR, Metzler CM, Charlton MD, Harmatz JS*, et al.* (1992). Pharmacokinetics and pharmacodynamics of oral diazepam: effect of dose, plasma concentration, and time. Clin Pharmacol Ther 52**:**139-150.

Fritschy JM, Benke D, Johnson DK, Mohler H, & Rudolph U (1997). $GABA_A$-receptor α-subunit is an essential prerequisite for receptor formation *in vivo* . Neuroscience 81**:** 1043-1053.

Frohlich J, Miller MT, Bird LM, Garces P, Purtell H, Hoener MC*, et al.* (2019a). Electrophysiological Phenotype in Angelman Syndrome Differs Between Genotypes. Biol Psychiatry 85**:** 752-759.

Frohlich J, Reiter LT, Saravanapandian V, DiStefano C, Huberty S, Hyde C*, et al.*(2019b). Mechanisms underlying the EEG biomarker in Dup15q syndrome. Mol Autism 10**:** 29.

Grabner G, Janke AL, Budge MM, Smith D, Pruessner J, & Collins DL (2006). Symmetric atlasing and model based segmentation: an application to the hippocampus in older adults. Med Image Comput Comput Assist Interv 9**:** 58-66.

Gunn RN, Lammertsma AA, Hume SP, & Cunningham VJ (1997). Parametric imaging of ligand-receptor binding in PET using a simplified reference region model. Neuroimage 6**:**279-287.

Hadingham KL, Wingrove P, Le Bourdelles B, Palmer KJ, Ragan CI, & Whiting PJ (1993). Cloning of cDNA sequences encoding human α2 and α3 gamma-aminobutyric acidA receptor subunits and characterization of the benzodiazepine pharmacology of recombinant α1-, α2-, α3-, and α5-containing human γ-aminobutyric $acid_A$ receptors. Molecular pharmacology 43**:**970-975.

Halldin C, Farde L, Litton JE, Hall H, & Sedvall G (1992). [^{11}C]Ro 15-4513, a ligand for visualization of benzodiazepine receptor binding. Preparation, autoradiography and positron emission tomography. Psychopharmacology (Berl) 108**:** 16-22.

Hipp JF, & Siegel M (2013). Dissociating neuronal gamma-band activity from cranial and ocular muscle activity in EEG. Front Hum Neurosci 7**:** 338.

Jenkinson M, Pechaud M, & Smith S BET2: MR-based estimation of brain, skull and scalp surfaces.

Kawaharada S, Nakanishi M, Nakanishi N, Hazama K, Higashino M, Lewis A*, et al.* (2018). ONO-8590580, a novel $GABA_A$ α5 negative allosteric modulator enhances long-term potentiation and improves cognitive deficits in preclinical models. J Pharmacol Exp Ther 366**:** 58-65.

Lake EM, Chaudhuri J, Thomason L, Janik R, Ganguly M, Brown M*, et al.* (2015). The effects of delayed reduction of tonic inhibition on ischemic lesion and sensorimotor function. J Cereb Blood Flow Metab 35**:** 1601-1609.

Lammertsma AA, & Hume SP (1996). Simplified reference tissue model for PET receptor studies. Neuroimage 4**:** 153-158.

Li M, Szabo A, & Rosenberg HC (2001). Evaluation of native $GABA_A$ receptors containing an α5 subunit. Eur J Pharmacol 413**:** 63-72.

Little HJ, Nutt DJ, & Taylor SC (1984). Acute and chronic effects of the benzodiazepine receptor ligand FG 7142: proconvulsant properties and kindling. Br J Pharmacol 83**:** 951-958.

Loscher W (2009). Preclinical assessment of proconvulsant drug activity and its relevance for predicting adverse events in humans. Eur J Pharmacol 610**:** 1-11.

Maeda J, Suhara T, Kawabe K, Okauchi T, Obayashi S, Hojo J*, et al.* (2003). Visualization of α5 subunit of $GABA_A$/benzodiazepine receptor by [^{11}C] Ro15-4513 using positron emission tomography. Synapse 47**:** 200-208.

Malherbe P, Bissantz C, Marcuz A, Kratzeisen C, Zenner MT, Wettstein JG*, et al.* (2008). Me-talnetant and osanetant interact within overlapping but not identical binding pockets in the human tachykinin neurokinin 3 receptor transmembrane domains. Molecular pharmacology 73**:** 1736-1750.

Malizia AL, Gunn RN, Wilson SJ, Waters SH, Bloomfield PM, Cunningham VJ*, et al.* (1996). Benzodiazepine site pharmacokinetic/pharmacodynamic quantification in man: direct measurement of drug occupancy and effects on the human brain in vivo. Neuropharmacology 35**:** 1483-1491.

Martinez-Cue C, Martinez P, Rueda N, Vidal R, Garcia S, Vidal V*, et al.* (2013). Reducing $GABA_A$ α5 receptor-mediated inhibition rescues functional and neuromorphological deficits in a mouse model of down syndrome. J Neurosci 33**:** 3953-3966.

Maubach K (2003). $GABA_A$ receptor subtype selective cognition enhancers. Curr Drug Targets CNS Neurol Disord 2**:** 233-239.

McGinnity CJ, Riano Barros DA, Rosso L, Veronese M, Rizzo G, Bertoldo A*, et al.* (2017). Test-retest reproducibility of quantitative binding measures of [^{11}C]Ro15-4513, a PET ligand for $GABA_A$ receptors containing alpha5 subunits. Neuroimage 152**:** 270-282.

McKernan RM, Quirk K, Prince R, Cox PA, Gillard NP, Ragan CI*, et al.* (1991). $GABA_A$receptor subtypes immunopurified from rat brain with α subunit-specific antibodies have unique pharmacological properties. Neuron 7**:**667-676.

McNaughton N, & Morris RG (1987). Chlordiazepoxide, an anxiolytic benzodiazepine, impairs place navigation in rats. Behavioural brain research 24**:** 39-46.

Merschman SA, Rose MJ, Pearce GE, Woolf EJ, Schaefer BH, Huber AC*, et al.* (2005). Characterization of the solubility of a poorly soluble hydroxylated metabolite in human urine and its implications for potential renal toxicity. Pharmazie 60**:** 359-363.

Miller RG (1974). The jackknife-a review. Biometrika 61**:** 1-15.

Morris R (1984). Developments of a water-maze procedure for studying spatial learning in the rat. Journal of neuroscience methods 11**:** 47-60.

Myers JF, Comley RA, & Gunn RN (2017). Quantification of [^{11}C]Ro15-4513 $GABA_A$α5 specific binding and regional selectivity in humans. J Cereb Blood Flow Metab 37**:** 2137-2148.

Nichols TE, & Holmes AP (2002). Nonparametric permutation tests for functional neuroimaging: a primer with examples. Hum Brain Mapp 15**:** 1-25.

Nicolas LB, & Prinssen EP (2006). Social approach-avoidance behavior of a high-anxiety strain of rats: effects of benzodiazepine receptor ligands. Psychopharmacology (Berl) 184**:** 65-74.

Olsen RW, & Sieghart W (2009). $GABA_A$ receptors: Subtypes provide diversity of function and pharmacology. Neuropharmacology 56**:** 141-148.

Pirker S, Schwarzer C, Wieselthaler A, Sieghart W, & Sperk G (2000). $GABA_A$ receptors: immunocytochemical distribution of 13 subunits in the adult rat brain. Neuroscience 101**:** 815-850.

Porjesz B, Almasy L, Edenberg HJ, Wang K, Chorlian DB, Foroud T*, et al.* (2002). Linkage disequilibrium between the beta frequency of the human EEG and a $GABA_A$ receptor gene locus. Proc Natl Acad Sci U S A 99**:** 3729-3733.

Povroznik JM, Rudy CC, Hunsberger HC, Tosto DE, & Reed MN (2014). Effects of an α5$GABA_A$inverse agonist on MK-801-induced learning deficits in an incremental repeated acquisition task. Behav Pharmacol 25**:** 331-335.

Quirk K, Blurton P, Fletcher S, Leeson P, Tang F, Mellilo D*, et al.* (1996). [^{3}H]L-655,708, a novel ligand selective for the benzodiazepine site of $GABA_A$ receptors which contain the α5 subunit. Neuropharmacology 35**:** 1331-1335.

Redrobe JP, Elster L, Frederiksen K, Bundgaard C, de Jong IE, Smith GP*, et al.* (2012). Negative modulation of $GABA_A$ α5 receptors by RO4938581 attenuates discrete sub-chronic and early postnatal phencyclidine (PCP)-induced cognitive deficits in rats. Psychopharmacology (Berl) 221**:**451-468.

Rudolph U, & Knoflach F (2011). Beyond classical benzodiazepines: novel therapeutic potential of $GABA_A$ receptor subtypes. Nat Rev Drug Discov 10**:** 685-697.

Rutten K, Basile JL, Prickaerts J, Blokland A, & Vivian JA (2008). Selective PDE inhibitors rolipram and sildenafil improve object retrieval performance in adult cynomolgus macaques. Psychopharmacology (Berl) 196**:** 643-648.

Savic MM, Clayton T, Furtmuller R, Gavrilovic I, Samardzic J, Savic S*, et al.* (2008). PWZ-029, a compound with moderate inverse agonist functional selectivity at $GABA_A$ receptors containing α5 subunits, improves passive, but not active, avoidance learning in rats. Brain Res 1208**:** 150-159.

Schmidt S, Bruehl C, Frahm C, Redecker C, & Witte OW (2012). Age dependence of excitatory-inhibitory balance following stroke. Neurobiol Aging 33**:** 1356-1363.

Sieghart W, & Savic MM (2018). International Union of Basic and Clinical Pharmacology. CVI: $GABA_A$ Receptor Subtype- and Function-selective Ligands: Key Issues in Translation to Humans. Pharmacol Rev 70**:** 836-878.

Sigel E, & Steinmann ME (2012). Structure, function, and modulation of $GABA_A$ receptors. J Biol Chem 287**:** 40224-40231.

Smit DJA, Wright MJ, Meyers JL, Martin NG, Ho YYW, Malone SM*, et al.* (2018). Genome-wide association analysis links multiple psychiatric liability genes to oscillatory brain activity. Hum Brain Mapp 39**:** 4183-4195.

Smith SM, Jenkinson M, Woolrich MW, Beckmann CF, Behrens TE, Johansen-Berg H*, et al.* (2004). Advances in functional and structural MR image analysis and implementation as FSL. Neuroimage 23 Suppl 1**:** S208-219.

Stillhart C, Parrott NJ, Lindenberg M, Chalus P, Bentley D, & Szepes A (2017). Characterising Drug Release from Immediate-Release Formulations of a Poorly Soluble Compound, Basmisanil, Through Absorption Modelling and Dissolution Testing. AAPS J 19**:** 827-836.

Sur C, Fresu L, Howell O, McKernan RM, & Atack JR (1999). Autoradiographic localization of α5 subunit-containing $GABA_A$ receptors in rat brain. Brain Res 822**:** 265-270.

Timic Stamenic T, Joksimovic S, Biawat P, Stankovic T, Markovic B, Cook JM*, et al.* (2015). Negative modulation of α5 $GABA_A$ receptors in rats may partially prevent memory impairment induced by MK-801, but not amphetamine- or MK-801-elicited hyperlocomotion. Journal of psychopharmacology (Oxford, England) 29**:** 1013-1024.

Traub RD, Jefferys JGR, & Whittington MA (1999) *Fast oscillations in cortical circuits* . The MIT Press: Cambridge, MA.

Tziortzi AC, Searle GE, Tzimopoulou S, Salinas C, Beaver JD, Jenkinson M*, et al.* (2011). Imaging dopamine receptors in humans with [^{11}C]-(+)-PHNO: dissection of D3 signal and anatomy. Neuroimage 54**:** 264-277.

Visser SA, Wolters FL, van der Graaf PH, Peletier LA, & Danhof M (2003). Dose-dependent EEG effects of zolpidem provide evidence for $GABA_A$ receptor subtype selectivity in vivo. J Pharmacol Exp Ther 304**:** 1251-1257.

Whittington MA, Traub RD, Kopell N, Ermentrout B, & Buhl EH (2000). Inhibition-based rhythms: experimental and mathematical observations on network dynamics. Int J Psychophysiol 38**:** 315-336.

Zanos P, Nelson ME, Highland JN, Krimmel SR, Georgiou P, Gould TD*, et al.* (2017). A Negative Allosteric Modulator for α5 Subunit-Containing GABA Receptors Exerts a Rapid and Persistent Antidepressant-Like Action without the Side Effects of the NMDA Receptor Antagonist Ketamine in Mice. eNeuro 4.

Zurek AA, Yu J, Wang DS, Haffey SC, Bridgwater EM, Penna A*, et al.* (2014). Sustained increase in α5$GABA_A$ receptor function impairs memory after anesthesia. J Clin Invest 124**:** 5437-5441.

Figure Legends

Figure 1. Chemical structure of basmisanil: RO5186582; RG1662; C21H20FN3O5S; molecular weight 445.469; 1,1-Dioxo-1,6-thiomorpholin-4-yl)-{6-[3-(4-fluoro-phenyl)-5-methyl-isoxazol-4-ylmethoxy]-pyridin-3-yl}-methanone.

Figure 2 . Basmisanil is a potent and highly selective $GABA_A$-α5 receptor NAM.

Data in the graphs are shown as mean (symbols) ± SEM (error bars). Error bars smaller than the symbol size are not shown.

(**A**) Concentration-response curves of basmisanil in [^{3}H]-flumazenil competition-binding assays to membranes expressing different human recombinant $GABA_A$receptor subtypes (n = 7-9 per concentration). (**B**) Concentration-response curves of the effects of basmisanil on ion current induced by an EC_{10} of GABA in Xenopus oocytes (n = 3-12 per concentration). (**C**) and (**D**) Flumazenil antagonism of basmisanil effects. (**C**) Example recording of ion current from a voltage-clamped Xenopus oocyte expressing human $GABA_A$-α5. Two current traces are superimposed. The control response (black) was evoked by a GABA application in the absence of any modulators, as indicated by the black horizontal bar. During the test response (blue), after a delay, basmisanil and then flumazenil (blue horizontal bars) were added to GABA. (**D**) Bar graph showing flumazenil antagonism of the basmisanil effect. Green bars: flumazenil alone (30 nM: n = 5, 1000 nM: n = 11). Blue bars: flumazenil in presence of basmisanil (100 nM basmisanil: n = 16; basmisanil + flumazenil 30 nM: n = 6; basmisanil + flumazenil 1000 nM: n = 10).

Figure 3. Dose-dependent $GABA_A$-α5 receptor occupancy by basmisanil in rat brain.

Dose-dependent blockade of [^{3}H]-Ro 15-4513 binding by basmisanil determined 60 min after p.o. administration of basmisanil and 15 min after i.v. injection of [^{3}H]-Ro 15-4513. (**A**) Sagittal brain sections of female Sprague-Dawley rats pretreated with vehicle (n = 4), L-655,708 (10 mg kg^{-1}; n = 4) or increasing

doses of basmisanil at 3 mg kg^{-1} (n = 4), 10 mg kg^{-1} (n = 4), 30 mg kg^{-1}(n = 4) and 100 mg kg^{-1} (n = 2). (**B**) Quantitative autoradiography signals in the hippocampus were plotted against individual plasma concentrations of basmisanil. The curve was fitted to the experimental results using the Hill equation (equation 1 with Hill coefficient D = 1).

Figure 4. Basmisanil improved cognition in rodents and non-human primates.

(**A**) Basmisanil reversed the diazepam-induced spatial learning impairment of rats in the Morris water maze. Basmisanil (3 and 10 mg kg^{-1} p.o. as indicated below the abscissa) and diazepam (6 mg kg^{-1} i.p.) were administered to male Lister Hooded rats 30 min before the test. Data are presented as mean ± SEM (n = 10 per dose group). Bars indicate the percent of time spent in the left (dotted), platform (black), right (plain) and opposite (hatched) quadrants. Statistics: * significant difference between vehicle and diazepam-treated groups on percent time in platform quadrant (unpaired t-test); # significant difference between percent time spent in platform quadrant versus left, right and opposite quadrants (post hoc Newman-Keuls test).

(**B**) Basmisanil improved executive function in adult cynomolgus macaques. The effect of basmisanil administered at 1, 3, 10 and 30 mg kg^{-1} p.o. on percent correct (first reaches) during difficult trials of the object retrieval task. Data are presented as mean ± SEM (n = 12/dose; within-subjects design). Statistics: * significant difference versus vehicle-treated group (post hoc Dunnett's test).

Figure 5. Mean free plasma exposures achieved with basmisanil in the cognition tests, Morris water maze (MWM; n = 4) and object retrieval (OR; n = 3), proconvulsant test (PTZ; n = 8) and anxiety test (SAA; n = 4) and the relationship to $GABA_A$-α5 receptor occupancy. Squares: free plasma concentration for MWM, OR and EC_{50} receptor occupancy. Open circles: exposures with negative outcome in the test. Closed circle: pro-convulsant activity in 5/8 rats.

Figure 6. Dose-dependent $GABA_A$-α5 receptor occupancy by basmisanil in human brain.

(**A**) Representative [^{11}C]-Ro 15-4513 PET images in healthy human subjects showing the $GABA_A$-α5 receptor distribution. BP_{ND} = binding potential; SRTM = simplified reference tissue model; Cb = cerebellum. Numbers for each slice indicate the axial slice location in MNI coordinates. (**B**) Relation between basmisanil concentration in plasma and receptor occupancy derived from nine subjects. Emax model fit (E=Emax*C/(EC_{50}+C)), gray band indicates 95% confidence interval determined by the profile likelihood method. Blue and red bars indicate mean ± SD of blood plasma concentrations in the EEG experiment at 1 h and 4 h post morning dose at day 14, respectively.

Figure 7. Electrophysiological signature of basmisanil in healthy volunteers.

(**A**) Relative power change of EEG signals averaged across all electrodes compared to baseline recording for basmisanil (blue band: eyes open & eyes closed, 1 h and 4 h post morning dose after 14 days of treatment) and midazolam (grey band: eyes open & eyes closed, 1 h post single dose) in twelve healthy subjects. Black bars indicate significant effects for basmisanil (cluster randomization test). CI = confidence interval. (**B**) Spatial distribution of power changes and P-values (derived from t-tests) for the two significant clusters identified for basmisanil (black bars in A). Top panel: power changes; bottom panel: P-values; left: low-frequency cluster (6.2–8.7 Hz); right: high-frequency cluster (13.5-38.0 Hz). See Supporting Figure S5 for additional analyses.

Figure 1

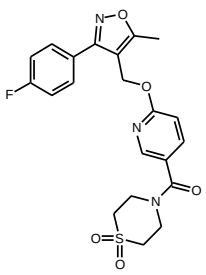

1

Figure 2

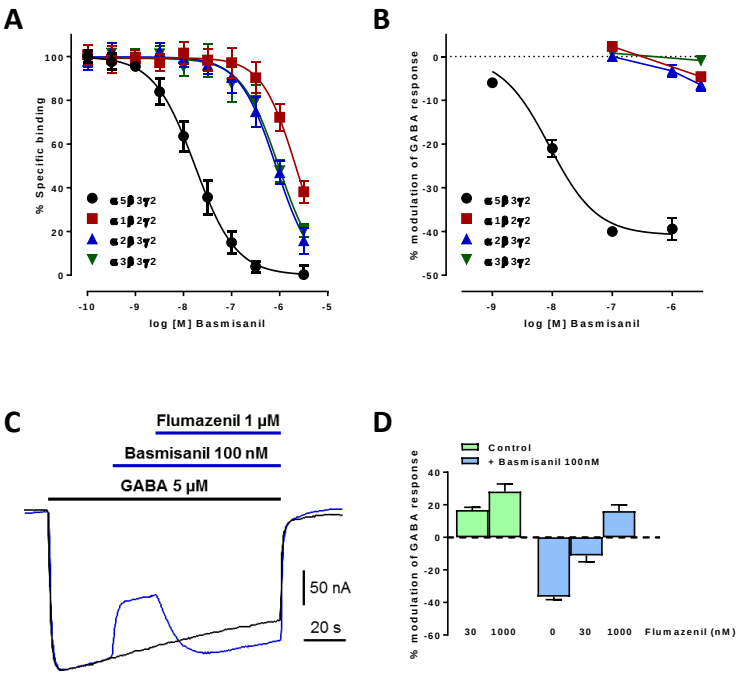

Figure 3

A

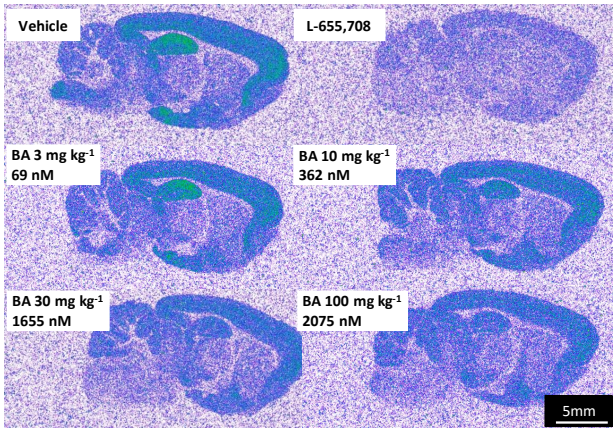

B

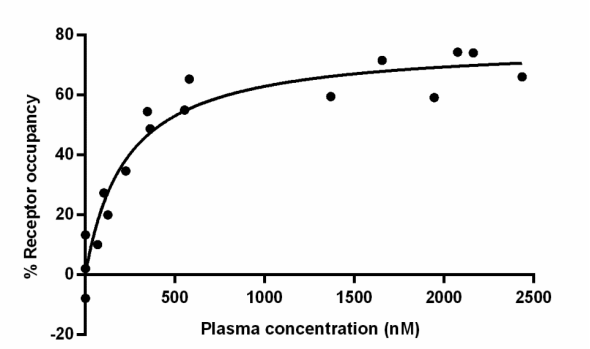

1

Figure 4

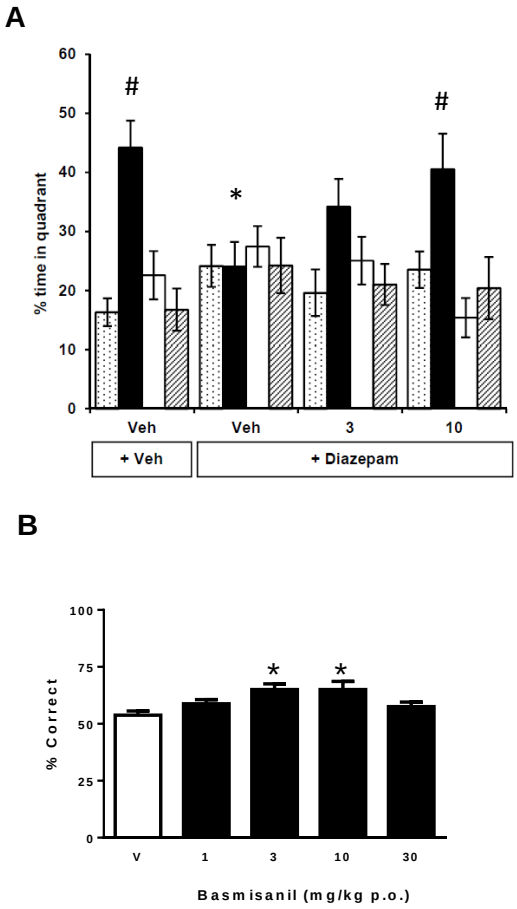

Figure 5

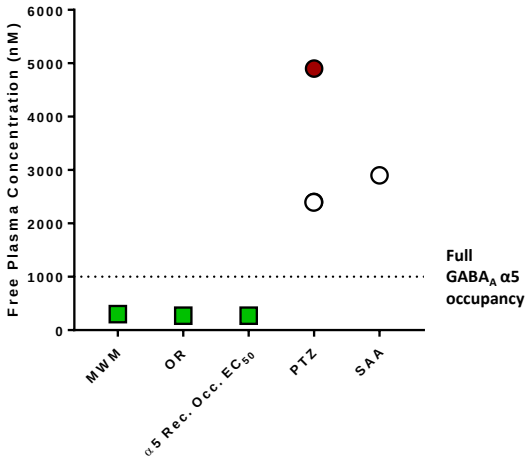

1

Figure 6

A

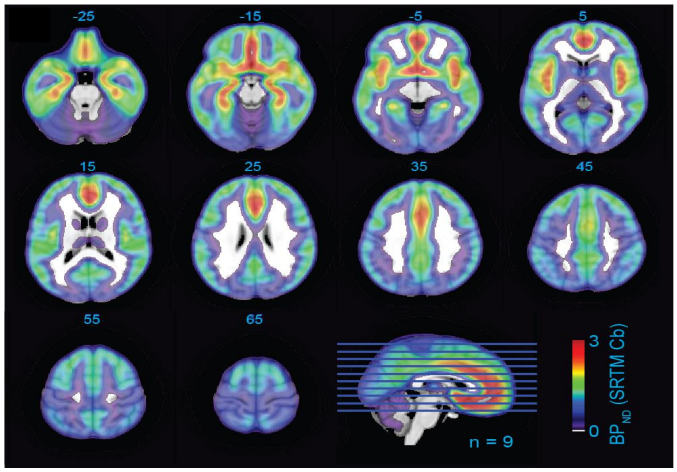

B

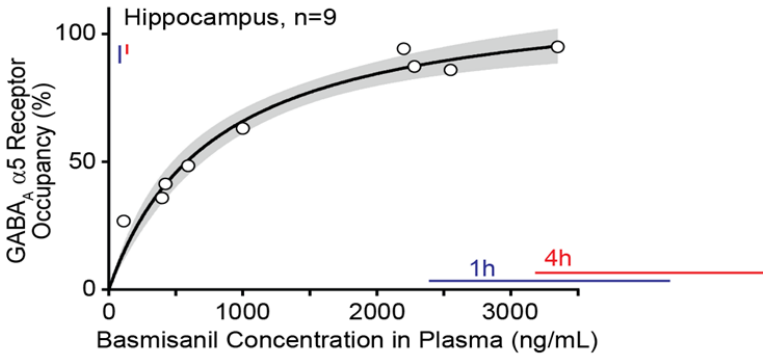

1

Figure 7

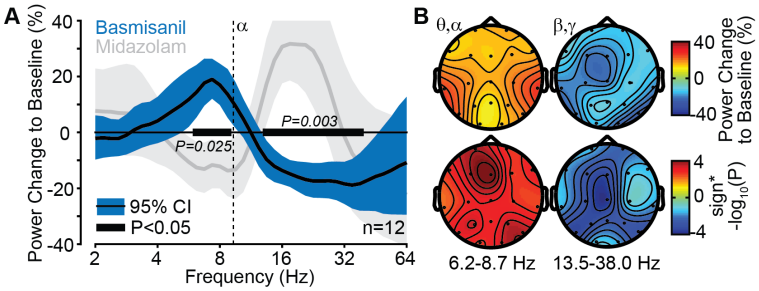

1

Table 1. Basmisanil exhibits binding and functional selectivity for the human $GABA_A$-α5 receptor subtype in vitro

Human $GABA_A$ receptor subtype	Binding affinity [a] Ki (nM) ± SEM	$GABA_A$ receptor inhibition IC_{50} (nM) [b] (Modulation of GABA EC_{10} ± SEM)
α1β3γ2	1030.8 ± 54.3	> 3000[c] (-4.6 ± 0.8%)
α2β3γ2	457.7 ± 27.2	> 3000[c] (-6.5 ± 1.4%)
α3β3γ2	509.6 ± 20.7	> 3000[c] (-0.9 ± 0.4%)
α5β3γ2	5.07 ± 0.7	8.6 (–39.4 ± 2.5%)

[a] Inhibition by basmisanil of [^{3}H]-flumazenil binding to recombinant human $GABA_A$ α1 (n = 9), α2 (n = 9), α3 (n = 7), and α5 (n = 8) subunit-containing receptor subtypes.

[b] Inhibition by basmisanil of the ion current evoked by submaximal GABA concentrations (EC_{10}) in Xenopus laevis oocytes expressing recombinant human $GABA_A$ receptor subtypes (n = 3-12 oocytes per concentration). The maximum degree of inhibition of α5β3γ2 evoked by 1000 nM basmisanil was –39.4 ± 2.5% (n = 7).

[c] <10% inhibition at 3000 nM.